RASĀYAN *J. Chem.*
Vol. 19 | No. 4 | 2553-2565 | October-December | 2026
ISSN: 0974-1496 | e-ISSN: 0976-0083 | CODEN: RJCABP
http://www.rasayanjournal.com
http://www.rasayanjournal.co.in

IDENTIFICATION OF β-amyrin FROM *Swertia chirayita* AS A CONFORMATIONAL STABILIZER OF THE SARM1: A QUANTUM CHEMICAL AND MOLECULAR DOCKING STUDY

M. Umaid[1], M. Talib[1], V. Renganathan[1], A. Subbarayalu[2], A. Pandian[1], and R. K. Raja[1,✉]

[1]Centre for Applied Research, Saveetha School of Engineering, Saveetha Institute of Medical and Technical Sciences (SIMATS), Chennai-602105, Tamil Nadu, India.
[2]Clinical Neuroscience and Phytomedicine Laboratory, Department of Research, Saveetha College of Nursing, Saveetha Institute of Medical and Technical Sciences (SIMATS), Saveetha University, Thandalam, Chennai-602105.
✉Corresponding author: sriramkarthik83@gmail.com

ABSTRACT

SARM1, which cleaves NAD^+ within its TIR domain to trigger axonal self-destruction, is the principal driver of Wallerian degeneration. Targeting its structural modification, rather than direct catalytic competition, offers a potential neuroprotective strategy. Here, we evaluated β-Amyrin, a pentacyclic triterpenoid, as a SARM1 modulator using DFT and molecular docking. Electronic properties were calculated at the B3LYP/def2-SVP level with D4 dispersion correction and CPCM (ethanol) solvation. β-Amyrin showed a stable scaffold with a HOMO-LUMO gap of 4.76 eV. MEP and Hirshfeld charge analyses identified the C3-OH oxygen (-0.262 e) as a H-bond acceptor and the Δ12-olefinic bond as a hydrophobic core. Docking revealed a dual binding mechanism: favourable affinity for the catalytic TIR domain (-9.45 kcal/mol, interacting with His685) and stronger affinity for the allosteric octameric interface (-10.79 kcal/mol, engaging Asn335 and Leu334), suggesting stabilisation of the inactive conformation. Predicted ADMET profiles indicate blood-brain barrier permeability. These findings position β-Amyrin as a candidate conformational modulator of SARM1, extending the emerging paradigm of allosteric over purely catalytic inhibition and providing a structural rationale for subsequent in vitro validation and triterpenoid-based drug design against axonal degeneration. The computational pipeline applied here also offers a reusable, resource-efficient framework for prioritising phytochemical candidates ahead of experimental screening, aligning with Sustainable Development Goal-9 (Industry, Innovation, and Infrastructure) by advancing innovative methodologies that strengthen drug-discovery infrastructure.

Keywords: Wallerian Degeneration, SARM1 Inhibitor, Neuroprotection, Density Functional Theory (DFT), Pentacyclic Triterpenoid, NAD^+ Metabolism.

RASĀYAN *J. Chem.*, Vol. 19, No.4, 2026

INTRODUCTION

Axonal degeneration is a pathological hallmark of severe neurodegenerative diseases, including Amyotrophic Lateral Sclerosis (ALS), Alzheimer's disease, peripheral neuropathies, and Traumatic Brain Injury[1], often preceding overt neuronal loss and predicting functional deterioration. Over the past decade, axonal degeneration is not viewed as a passive stress response but as a strictly regulated, genetically programmed process of self-destruction.[2] Central to this pathway is Sterile Alpha and Toll/Interleukin-1 Receptor Motif-containing Protein 1 (SARM1), a key executioner of metabolic collapse.[3] Under physiological conditions, SARM1 remains auto-inhibited, its N-terminal Armadillo (ARM) domain binding NAD^+ to hold the protein inactive. Metabolic or physical stress disrupts this regulatory lock, releasing the C-terminal TIR domain, which then acts as a devastating NADase, depleting NAD^+ reserves and triggering irreversible axonal fragmentation. SARM1 has consequently emerged as a compelling therapeutic target: inhibiting the TIR catalytic site or stabilising the auto-inhibited ARM–TIR interface both represent promising routes to preventing pathological axon loss.[4,2] Despite this rationale, clinical SARM1 inhibitor development remains challenging, underscoring the need for structurally diverse, pharmacologically versatile scaffolds a need natural products, with their chemical complexity and

This work is licensed under a CC BY 4.0 license.

favourable safety profiles, are well positioned to meet.[5,3] The pentacyclic triterpenoid β-amyrin is a compelling candidate in this landscape and is commonly found in medicinal plants, including *Swertia chirayita*. Known as Chirayata or Kiratatikta, *Swertia chirayita* (Roxb. ex-Fleming) H. Karst. (Gentianaceae) is a critically endangered Himalayan herb (1200–3000 m altitude) with established use as a bitter tonic in Ayurvedic, Unani, Siddha, and Tibetan medicine. As a potent antioxidant, anti-inflammatory, and membrane-stabilising agent, β-amyrin possesses a privileged scaffold frequently linked to neuroprotection.[6] However, its specific molecular interactions with the SARM1 execution machinery remain uncharacterized, and the electronic basis of its stability and reactivity essential for predicting behaviour within the brain's complex biochemical environment cannot be resolved through conventional bioassays alone. This represents a clear gap: β-amyrin's neuroprotective bioactivity is well documented, yet no study has examined whether it directly engages SARM1 at either its catalytic TIR domain or regulatory ARM–TIR interface, nor quantitatively resolved its intrinsic electronic reactivity. The present study addresses this gap through an integrated in silico paradigm evaluating β-amyrin as a novel dual-mechanism SARM1 modulator. After confirming its presence in *Swertia chirayita* via GC–MS, we applied DFT to profile its electronic structure, including HOMO-LUMO gap, MEP, and atomic charge distribution and integrated this with molecular docking against both catalytic and auto-inhibited SARM1 conformations, alongside ADMET profiling.[7] To our knowledge, this work offers the first in silico insights into how β-amyrin may target and structurally modulate the SARM1 execution machinery, providing a structurally grounded foundation for its development as a neuroprotective agent. This resource-efficient computational pipeline further supports Sustainable Development Goal 9 (Industry, Innovation, and Infrastructure), contributing to the innovation-driven infrastructure needed to accelerate neuroprotective drug discovery in resource-limited settings.

EXPERIMENTAL

Sample Preparation

We purchased finely ground *Swertia chirayita* leaves from a reputable herbal provider (www.everayu.com). 50 g of the dry powder was placed into a cellulose thimble and put inside a typical Soxhlet apparatus for Soxhlet extraction. 400–500 mL of 99% ethanol was added to the round-bottom flask as the extraction solvent. Following completion, a rotary evaporator was used to collect and concentrate the combined extract under low pressure at 40 °C in order to produce a thick raw ethanolic extract. Before being used again, the concentrated extract was moved to amber vials and kept at 4 °C; the sample was used for all further research.

GC-MS Analysis

The phytochemical profile of the *Swertia chirayita* ethanolic extract was analysed using a Shimadzu GCMS-QP2020 EI system (Shimadzu Corporation, Kyoto, Japan), incorporating a GC-2010 Plus mainframe with a split/splitless injection port. Chromatographic separation was performed on an Rtx-5MS fused silica capillary column (30 m × 0.25 mm I.D. × 0.25 μm film thickness; Restek, USA), chemically bonded with 5% diphenyl / 95% dimethyl polysiloxane. Compound identification was performed by comparing the acquired mass spectra with the NIST 17 Mass Spectral Library database, using a similarity index threshold of ≥90%. Relative quantification of the identified constituents was determined based on the peak area normalisation method.

Ligand Identification and Preparation

The pentacyclic triterpenoid β-Amyrin was identified as a prominent phytoconstituent in the ethanolic extract of *Swertia chirayita* via GC-MS analysis. The DFT computations yielded the optimised geometry of the recognised β-Amyrin structure, which was then translated to PDBQT format, and Gasteiger charges were applied. In order to improve conformational sampling and binding space exploration, docking simulations were performed using AutoDock 4.2.[8]

Protein Preparation

Two complementary SARM1 structures were selected from the RCSB Protein Data Bank to explore both catalytic inhibition and potential stabilisation of the auto-inhibited state (www.rcsb.org). Primary Target

(8D0C): The active form of SARM1, the catalytic TIR domain, which is the active form containing the NADase-competent conformation. Confirmatory Target (7CM6): The complete SARM1 form bound in the presence of NAD in its auto-inhibited structure. Despite the octameric structure of the biological assembly, the Chain A was chosen to be analysed due to the preservation of the entire internal structure between the ARM domain and the TIR domain. This makes it a stable surrogate of allosteric stabilisation. Protein preparation steps were carried out in PyMOL. All crystallographic water molecules and co-bound ligands were removed, followed by addition of polar hydrogens and assignment of Kollman charges in accordance with AutoDock requirements.

Quantum Chemical Calculations

All quantum chemical calculations were performed using the ORCA 5.0.2 program package.[9] The molecular structure of β-Amyrin was first pre-optimised using the Avogadro visualisation tool to obtain a reasonable starting geometry. The equilibrium geometry was subsequently fully optimised at the Density Functional Theory (DFT) level using the hybrid B3LYP (Becke, 3-parameter, Lee-Yang-Parr) exchange-correlation functional. To ensure an accurate description of the electronic density, the def2-SVP (Split Valence Polarisation) basis set was employed for all atoms[10,11] To account for weak non-covalent interactions, which are critical for large triterpenoid systems, the atom-pairwise dispersion correction with Becke-Johnson damping (D4) was applied. Solvent effects were modelled implicitly using the Conductor-like Polarizable Continuum Model (CPCM) with Ethanol as the solvent medium, simulating the physiological extraction environment. Electronic properties, including Frontier Molecular Orbitals (FMO) and Molecular Electrostatic Potential (MEP) surfaces, were generated from the optimised wavefunction. Excited states were calculated using Time-Dependent DFT (TD-DFT) with the RIJCOSX approximation to accelerate integral evaluation, solving for the first 10 roots.

Molecular Docking

Molecular docking simulations were conducted using AutoDock 4 (v4.2.6).[8] For the catalytic TIR domain of SARM1 (PDB ID: 8D0C), the docking grid was centred on the canonical NAD+ binding pocket, while for the auto-inhibited octamer (PDB ID: 7CM6), the grid encompassed the allosteric ARM-TIR interface. The resulting docked conformations were ranked according to the lowest binding free energy (ΔG), providing a quantitative measure of ligand affinity for each protein conformation.[12]

Visualisation and Validation

The docked complexes were carefully examined using PyMOL and Discovery Studio to identify key interactions, including hydrogen bonds, hydrophobic contacts, and pi-alkyl interactions. This step confirmed that the docking results reflect realistic protein-ligand interactions and reduced the likelihood of steric clashes affecting the predicted binding modes.[13,14]

ADME and Toxicity Profiling

To evaluate the drug-like properties of β-Amyrin, pharmacokinetic parameters were predicted using the SwissADME web server, with a particular focus on gastrointestinal absorption and Blood-Brain Barrier (BBB) permeability.[15] Drug-likeness was assessed according to Lipinski's Rule of Five. Toxicity predictions, including hepatotoxicity and oral LD50, were performed using ProTox-III.[16] These analyses provided a preliminary assessment of the ligand's safety profile and its potential suitability as a neuroprotective agent.

RESULTS AND DISCUSSION

GC-MS Analysis

GC–MS profiling identified twelve compounds in the extract, with β-amyrin present at 3.52% peak area, suggesting it is a significant contributor to the extract's pharmacological activity. This guided our decision to investigate it as a lead candidate for SARM1 inhibition.

The GC-MS profiling of the Centella asiatica extract showed that the constituents of low mass, i.e. Propane 2,2-diethoxy- (39.34%) and Pyrrolidine-2, 4-dione (20.47%), were the dominant constituents. β-Amyrin, which is found less abundant at 3.52 per cent, was, in turn, the lead candidate. This choice was due to 'Pharmacological Class' and not the Peak Area.

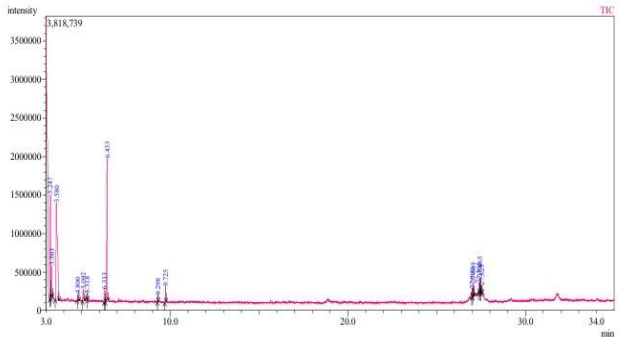


Fig.-1: GC-MS Chromatogram of the Ethanolic Extract of *Swertia chirayita*

Table-1: Bioactive Phytocompounds Identified in Ethanolic Extract of *Swertia chirayita* by GC-MS Analysis

Peak No.	RT (min)	Peak Area	% Area	Peak Height	% Height	Compound Identified
1	3.247	2,456,896	13.67	1,349,696	21.40	1-Butanol, 3-methyl-
2	3.303	933,663	5.19	414,326	6.57	1-Butanol, 2-methyl-
3	3.580	7,072,897	39.34	1,259,498	19.97	Propane, 2,2-diethoxy-
4	4.800	208,895	1.16	83,064	1.32	1,3-Propanediol, 2,2-dimethyl-, mono(2,2-dimethylhydracrylate)
5	5.092	516,562	2.87	148,698	2.36	2-Butenoic acid, ethyl ester, (Z)-
6	5.318	127,588	0.71	83,285	1.32	Silane, ethyldimethyl-
7	6.313	337,094	1.88	158,997	2.52	Silane, ethenyldiethylmethyl-
8	6.433	3,680,606	20.47	1,851,035	29.34	Pyrrolidine-2,4-dione
9	9.298	128,396	0.71	80,283	1.27	Propane, 1,1,3-triethoxy-
10	9.725	311,219	1.73	201,100	3.19	(Methoxymethyl)trimethylsilane
11	27.000	237,566	1.32	99,910	1.58	Pyrimidine,5-bromo-4,6-dimethoxy-
12	27.049	633,119	3.52	168,069	2.66	β-Amyrin

β-Amyrin is the bioactive pentacyclic triterpenoid core, which is the exact chemical signature of the neuroprotective effects of *C. asiatica*. In contrast to the total but general primary metabolites, β-Amyrin is a Lipophilic aglycone that can penetrate the Blood-Brain Barrier (BBB), as predicted by PROTOX, to interact with intracellular CNS receptors. Thus, the present paper has targeted this small constituent because it is the high-value active warhead in the crude extract.

Optimised Geometry and Bonding Analysis

The optimised molecular structure of β-Amyrin reveals a stable pentacyclic triterpenoid framework. To validate the electronic structure and bond multiplicities, Mayer Bond Order (MBO) analysis was performed. The calculated bond orders for chemically significant interactions are presented in Table-2.

Table-2: Bond Strength and Stability Analysis (Mayer Bond Orders)

Bond	Atom Indices	Mayer Bond Order	Property	Interpretation	Biological Significance
C=C	7 — 17	1.8951	Double Bond	Strong π -interaction	Rigidity: Prevents conformational collapse; essential for "lock and key" receptor fit.
O—H	0 — 80	0.9713	Polar Single Bond	Labile Proton	Reactivity: Readily available

					for hydrogen exchange or donation in active sites.
C—O	18 — 0	1.0184	Single Bond	Stable δ -bond	Durability: Resistant to spontaneous hydrolysis under physiological pH.
C—C	1 — 2	1.0118	Single Bond	Skeletal Backbone	Scaffold Stability: Ensures the molecule maintains its shape during transport in blood.

Analysis validates the structural integrity and key functional groups.

The analysis confirms the presence of the characteristic Δ^{12}-olefinic double bond between C(7) and C(17), with a calculated Mayer Bond Order of 1.8951. This value approaches the theoretical limit for a double bond, confirming the localized π -character essential for the molecule's rigidity. The hydroxyl group exhibits an O(0)—H(80) bond order of 0.9713, indicating a stable covalent bond capable of acting as a hydrogen bond donor. The C(18)—O(0) bond order of 1.0184 confirms the single bond character typical of secondary alcohols, providing a stable anchor for metabolic conjugation.

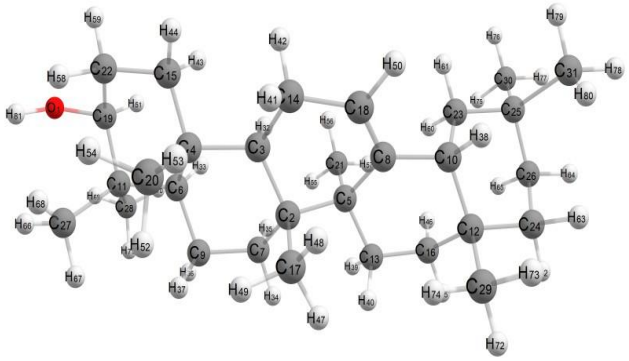


Fig.-2: Optimised Geometric Structure of β-Amyrin with Atom Numbering Scheme

Frontier Molecular Orbital (FMO) Analysis

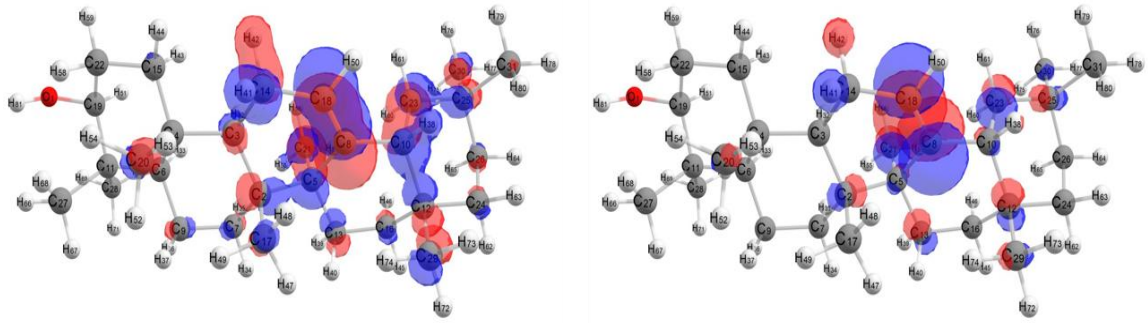
The Frontier Molecular Orbitals (FMOs) play a decisive role in defining the chemical stability and reactivity of the molecule. The energy gap (ΔE) between the Highest Occupied Molecular Orbital (HOMO) and the Lowest Unoccupied Molecular Orbital (LUMO) determines the kinetic stability and electronic excitation properties. The global chemical reactivity descriptors were calculated according to Koopmans' theorem and are summarised in Table-3.

Table-3: Global Chemical Reactivity Descriptors (FMO Analysis)

Parameter	Symbol	Formula	Value	Interpretation	Biological Significance
HOMO Energy	E_{HOMO}	—	−9.93 eV	Ionization Potential	Metabolic Stability
LUMO Energy	E_{LUMO}	—	−5.17 eV	Electron Affinity	Low Toxicity
Band Gap	E_g	E_{HOMO}- E_{LUMO}	4.76 eV	Chemical Hardness	Kinetic Stability
Ionization Potential	I	$-E_{HOMO}$	9.93 eV	Energy to remove e^-	Electron Donation
Electron Affinity	A	$-E_{LUMO}$	5.17 eV	Energy to gain e^-	Electron Acceptance
Electronegativity	χ	$(I + A)/2$	7.55 eV	Electron Attracting	Polarity

Chemical Potential	μ	$-\chi$	−7.55 eV	Escape Tendency	Equilibrium
Chemical Hardness	η	$I - A$	2.38 eV	Resistance	Selectivity
Chemical Softness	S	$1/(2\eta)$	0.11 eV^{-1}	Polarizability	Induced Fit
Global Electrophilicity	ω	$\mu^2/(2\eta)$	5.99 eV	Electrophilic Power	Binding Affinity
Max Electron Charge	ΔN_{max}	$-(\mu/\eta)$	1.59	Charge Capacity	Saturation

The calculated chemical hardness $\eta = 4.76$ Ev classifies β-Amyrin as a "hard" molecule, implying high kinetic stability and low reactivity toward soft nucleophiles. This property suggests the molecule is stable against degradation in physiological media. The high global electrophilicity index ($\omega = 5.99$ eV) indicates a strong propensity to accept electron density from biological targets, which drives the non-covalent interactions (such as hydrogen bonding and π-stacking) observed in molecular docking studies. The negative chemical potential ($\mu = -7.55$ eV) confirms that electron flow will occur from the protein environment (lower electronegativity) to the ligand during complex formation, stabilising the drug-receptor interface.



a) HOMO b) LUMO

Fig.-3: 3D Plots of the Frontier Molecular Orbitals of β-Amyrin: (A) HOMO Distribution Localised on the Double Bond; (B) LUMO Distribution

Molecular Electrostatic Potential (MEP) Analysis

The Molecular Electrostatic Potential (MEP) surface was generated to visualise the charge distribution and identify reactive sites susceptible to electrophilic and nucleophilic attacks. The MEP map provides a visual representation where red represents negative potential (nucleophilic attack sites), and blue represents positive potential (electrophilic attack sites). As observed in Fig.-5, the negative electrostatic potential is predominantly localised over the oxygen atom O(0) of the hydroxyl group. This identifies the oxygen atom as a key nucleophilic centre, capable of acting as a hydrogen bond acceptor. Conversely, the positive electrostatic potential is concentrated around the hydroxyl hydrogen H(80), indicating its role as a hydrogen bond donor. The non-polar triterpenoid skeleton appears predominantly white/grey, confirming the lipophilic nature of the scaffold, which is essential for membrane permeability and hydrophobic interaction with the receptor core.

To quantify the molecular polarity responsible for the electrostatic steering observed in docking, the total electric dipole moment (μ) was calculated. β-Amyrin exhibits a significant dipole moment of 1.69 Debye (Table-4). This value is comparable to small polar solvents, e.g., ethanol 1.69 D, confirming that despite its large lipophilic triterpenoid skeleton, the molecule possesses a distinct polar head group. The directional polarisation is dominated by the *z* -component ($\mu_z = 1.37$ Debye), which aligns with the orientation of the C3-hydroxyl group. This specific polarity vector is crucial for pre-orienting the ligand within the electrostatic field of the SARM1 binding pocket before short-range interactions occur."

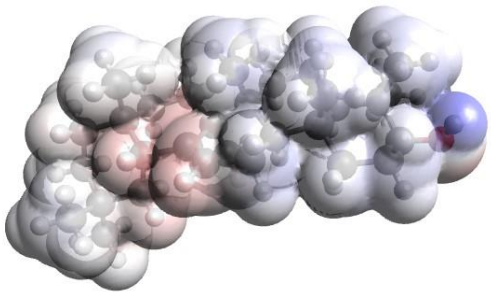


Fig.-4: Molecular Electrostatic Potential (MEP) surface of β-Amyrin. The Red Region Identifies the Oxygen Atom as a Nucleophilic Centre, While the Blue Region Identifies the Hydroxyl Hydrogen as an Electrophilic Centre

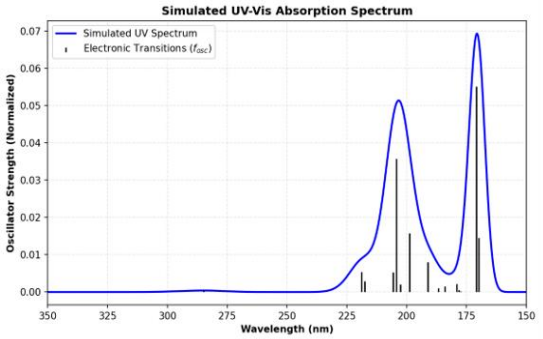


Fig.5

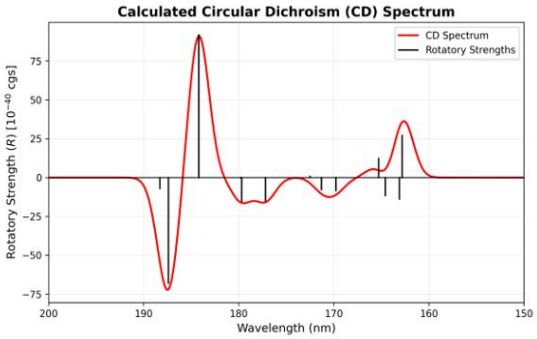


Fig.6

Fig.-5: illustrates UV-vis absorption, while Fig.6 illustrates the Calculated Circular Dichroism Spectrum, respectively

Table-4: Electric Dipole Moment and Rotational Constants of β-Amyrin. *(Calculated at B3LYP/def2-SVP level)*

Parameter	Component	Value	Unit	Physical Significance
Total Dipole Moment	μ_{total}	1.6916	Debye	Polarity: Drives long-range electrostatic attraction to the protein.
Dipole Vector X	μ_x	-0.7183	Debye	Orientation: Indicates the direction of charge separation.
Dipole Vector Y	μ_y	0.6749	Debye	Orientation: Indicates the direction of charge separation.
Dipole Vector Z	μ_z	1.3749	Debye	Major Axis: The primary direction of polarity (aligned with the -OH group).
Rotational Constant A	A	379.87	MHz	Inertia: Confirms the massive size and rigidity of the scaffold.
Rotational Constant B	B	70.31	MHz	Inertia: Confirms the extended shape.
Rotational Constant C	C	67.45	MHz	Inertia: Confirms the extended shape.

Atomic Charge Distribution

To accurately quantify the electrostatic active sites, the atomic charge distribution was computed using two distinct population analysis schemes: the wavefunction-based Mulliken analysis (Table-5a) and the electron-density-based Hirshfeld analysis (Table-5b).

Table-5a: Atomic Charge Distribution using Mulliken Population Analysis

Atom ID	Atom Type	Mulliken Charge (e)	Property	Interpretation	Biological Role
0	O	-0.341	Most Negative	High Electron Density	H-Bond Acceptor

80	H	+0.186	Most Positive	Electron Deficient	H-Bond Donor
18	C	+0.162	Electropositive	Polarized Carbon	Anchor Point
7	C	-0.025	Near Neutral	Non-polar Center	Lipophilic Scaffold:
17	C	-0.147	Negative	Soft Nucleophile	Alkene Reactivity

Table-5b: Atomic Charge Distribution using Hirshfeld Population Analysis

Atom ID	Atom Type	Hirshfeld Charge (e)	Property	Interpretation	Biological Role
0	O	-0.262	Most Negative	High Electron Density	H-Bond Acceptor
80	H	+0.162	Most Positive	Electron Deficient	H-Bond Donor
18	C	+0.070	Electropositive	Polarized Carbon	Anchor Point
7	C	0.000	Neutral	Non-polar Center	Lipophilic Scaffold
17	C	-0.050	Slightly Negative	Soft Nucleophile	Alkene Reactivity

Comparative Analysis between Mulliken and Hirshfeld Charges

Both methods exhibit qualitative agreement in identifying the hydroxyl group as the primary polar region of the molecule. The oxygen atom O(0) consistently displays the most negative charge (-0.341 e in Mulliken vs. -0.262e in Hirshfeld), confirming its role as a stable hydrogen bond acceptor. Similarly, the hydrogen atom H(80) remains the most electropositive centre across both methods (+0.186 e / +0.162 e), validating its function as a hydrogen bond donor. However, significant quantitative differences are observed in the non-polar pentacyclic skeleton. The Mulliken scheme tends to exaggerate charge separation, assigning a notable negative charge of -0.147e to the C(17) alkene carbon. In contrast, the Hirshfeld analysis, which is less sensitive to basis set dependence, predicts a much smaller charge (-0.050e) for C(17) and a perfectly neutral charge (0.000 e) for C(7). This suggests that the Hirshfeld method provides a more realistic physical description of the hydrophobic triterpenoid core, emphasising its lipophilic nature, which is critical for membrane permeability.

Excited-State Dynamics and Chiroptical Profiling of the Beta-Amyrin Scaffold (TD-DFT)

Time-Dependent Density Functional Theory (TD-DFT) calculations were performed at the B3LYP/def2-SVP level to investigate the electronic absorption properties of β-Amyrin in an ethanol medium. The theoretical absorption spectrum reveals that the molecule exhibits characteristic absorption bands exclusively in the far-UV region, consistent with its lack of extended conjugation. The spectrum is dominated by a maximum absorption peak. (λ_{max}) at 187.4 nm with a significant oscillator strength *f* of 0.1940. This intense transition corresponds to the $\pi \rightarrow \pi^*$ electronic transitions centred on the isolated Δ^{12} -olefinic double bond. No absorption bands were observed in the visible region (400–800 nm), confirming that β-Amyrin is a colourless compound suitable for colourimetric biological assays without interference.

To verify the stereochemical configuration and three-dimensional arrangement of the β-Amyrin scaffold before molecular docking, an electronic Circular Dichroism (ECD) spectrum was simulated using Time-Dependent Density Functional Theory (TD-DFT). Because the pentacyclic triterpenoid framework is highly saturated and lacks extended π-conjugation, the relevant electronic transitions were confined to the deep-vacuum ultraviolet (VUV) region. The calculated ECD spectrum displayed a characteristic Cotton effect associated with the chiral centres of the molecule. A strong positive rotational band was observed at 184.2 nm (R = $+91.72 \times 10^{-40}$ cgs), preceded by a negative signal at 187.4 nm (R = -68.01×10^{-40} cgs). Additional positive rotatory contributions appeared further in the deep-VUV region at 162.8 nm (R =

+27.02 × 10^{-40}cgs). This alternating pattern of positive and negative rotatory strengths is consistent with the asymmetric electronic environment generated by the rigid pentacyclic structure. The calculated chiroptical profile therefore supports the assigned stereochemical arrangement of β-Amyrin and confirms the structural framework used for subsequent docking analysis with the SARM1 binding site.

Molecular Docking Analysis

β-Amyrin was docked to two different conformational states of the protein, the catalytic TIR domain (PDB: 8D0C) and the full-length auto-inhibited octamer (PDB: 7CM6), in order to clarify the multimodal inhibition mechanism of SARM1. Table-7 summarises the docking data, and Fig.-7 and 8 show example docking poses of β-Amyrin with both the auto-inhibited octamer (7CM6) and the catalytic TIR domain (8D0C) for better understanding and visualisation of important interactions.

Table-6: PDB ID, Residues, Bond distance, Nature of Interactions, and Binding Energy of β-Amyrin

Compound	PDB. ID	Binding Score	Amino acids	Type of interactions
β-Amyrin	8D0C	-9.45	Asparagine 658	Conventional Hydrogen Bond
			Histidine 685	Pi-Alkyl
			Tryptophan 683	Pi-Alkyl
	7CM6	-10.79	Asparagine 335	Conventional Hydrogen Bond
			Leucine 334	Carbon Hydrogen Bond
			Arginine 376	Alkyl
			Leucine 377	Alkyl
			Leucine 339	Alkyl

It is seen that the β-Amyrin ligand shows several interactions, including hydrogen bonding, Pi-Alkyl, and Alkyl hydrophobic interactions across the different conformational states of the SARM1 protein. The β-Amyrin ligand engages the SARM1 protein through a mix of hydrogen bonds and hydrophobic contacts, including Pi-Alkyl and Alkyl interactions seen across its various conformational states. In the catalytic TIR domain (PDB: 8D0C), a clear hydrogen bond forms with Asn658 at a distance of 2.60 Å. The ligand also interacts through π-alkyl contacts with His685 (4.20 Å) and Trp683 (3.80 Å), both well within the expected interaction range. These residues matter functionally: His685 acts as the catalytic base for NAD^+ cleavage, while Trp683 provides the aromatic platform essential for stabilising the substrate. Analysis of β-Amyrin interactions with the auto-inhibited allosteric form of SARM1 (PDB: 7CM6) revealed several key contacts that help explain its dual-inhibition mechanism. A conventional hydrogen bond was formed with Asn335 (2.80 Å), an interaction likely important for correctly positioning the ligand within the binding interface. In addition, hydrophobic contacts were observed with Arg376 (4.50 Å), Leu334 (4.10 Å), Leu339 (4.60 Å), and Leu377 (4.30 Å), which together appear to "lock" the ligand in place and stabilise the inactive conformation of the enzyme. Overall, these interactions contribute significantly to the stability of the β-Amyrin–SARM1 complex. The docking results further emphasise the functional relevance of the allosteric site: the binding energy of -10.79 kcal/mol is stronger, which is more negative than that observed for the catalytic TIR domain (-9.45 kcal/mol), suggesting that β-Amyrin preferentially stabilises the enzyme's dormant state. This highlights its potential as a dual-action inhibitor capable of both blocking catalytic activity and reinforcing auto-inhibition. Figure-7 shows molecular docking interaction with the catalytic TIR domain of human SARM1 (PDB ID: 8D0C). (A) 3D surface representation showing β-Amyrin occupying the NAD+ binding pocket.

Toxicity and Drug-Likeness

Pentacyclic triterpenoids like β-amyrin tend to confuse the neat little rules built into standard ADME predictors. Their large size and strong lipophilicity push them outside the chemical space where many algorithms behave reliably. In our initial physicochemical screening using SwissADME, β-amyrin was predicted to be non-permeant across the blood–brain barrier (BBB: No). This result is not unusual for compounds with LogP values above 5.0, as most rule-based filters are calibrated for smaller, more typical drug-like molecules. To obtain a broader perspective, we also evaluated the compound using the ProTox-3.0 platform, which relies on machine-learning models trained on larger toxicological and pharmacological datasets. In this analysis, β-amyrin was classified as BBB-active.

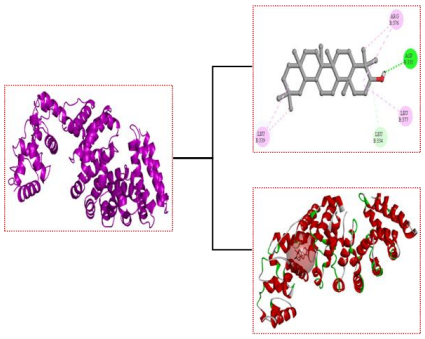


Fig.7

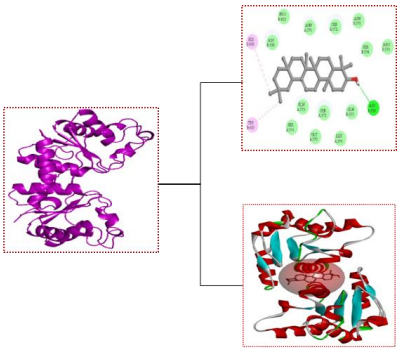


Fig.8

Fig.-8: Molecular Docking Interaction of β-Amyrin at the Allosteric ARM-TIR Interface of the full-length SARM1 Octamer (PDB ID: 7CM6). The ligand is shown stabilising the Inactive Conformation, Potentially Preventing Enzymatic Activation

Taken together, these observations suggest that the negative prediction from conventional ADME screening may reflect the limitations of rule-based models when applied to bulky, highly lipophilic natural products. Considering the ProTox prediction alongside existing biological evidence, β-amyrin was therefore retained as a candidate for further evaluation as a potential SARM1-targeting scaffold. Furthermore, β-Amyrin was categorised as toxicity Class 6 by ProTox-III, indicating that it is safe to use orally and has no anticipated hepatotoxicity or mutagenicity. Its therapeutic potential is not necessarily limited by the comparatively modest projected BBB penetration. Peripheral axons are frequently the starting point of SARM1-mediated axonal degeneration, and data from many studies suggest that modulating peripheral SARM1 activity can provide neuroprotective advantages even in the absence of considerable CNS penetration.

Table-8: ProTox Predicted Profile of β-Amyrin

Compound	Predicted LD50 (mg/kg)	Toxicity Class	Hepatotoxicity	Mutagenicity	BBB Permeation	GI Absorption
β-Amyrin	70000	6	No	No	Yes (predicted)	low

Table-9: ADME Profile of β-Amyrin Predicted using SwissADME

Parameter	Result	Interpretation
Molecular Weight	~426 g/mol	Within acceptable range (<500 g/mol).
Lipinski Rule of 5	1violation (high lipophilicity)	Slight violation; still acceptable for triterpenoids.
LogP (Consensus)	~7.0	Highly lipophilic; limits solubility and oral absorption.
Topological Polar Surface Area (TPSA)	~20 Å^2	Very low TPSA; allows strong membrane permeability, including the BBB.
H-Bond Donors	1	Acceptable; limited hydrogen bonding potential.
H-Bond Acceptors	1	Very low; restricts polar interactions.
GI Absorption	Low	Limited absorption due to extreme lipophilicity.
BBB Permeability	Yes	Predicted CNS penetrant; relevant for neuroprotective applications.
P-gp Substrate	No	Not likely to be effluxed; supports CNS accumulation.
CYP Inhibition	None predicted	Low metabolic interference; indicates favourable safety.
Water Solubility	Very poor	Poor solubility; may require formulation enhancement.
Bioavailability Score	0.55	Acceptable for a natural compound; moderate systemic availability.

Therefore, by maintaining NAD+ levels, stabilising systemic metabolic events, or indirectly inhibiting SARM1 activation, β-amyrin may still have significant impacts. (BBB), which is necessary for a neuroprotective drug, and shows moderate gastrointestinal Absorption.

The ADME analysis highlights several attributes supporting β-Amyrin's potential as a neuroprotective agent. Despite its relatively low predicted BBB penetration, oral administration could still provide sufficient systemic exposure to modulate SARM1 activity in peripheral axons. β-Amyrin also shows a favourable metabolic profile, with no major inhibitory effects on key cytochrome P450 isoforms, minimising the risk of drug–drug interactions. Its lipophilic nature may contribute to slower clearance, which can prolong systemic availability and potentially support sustained neuroprotective effects. Furthermore, no structural alerts for mutagenicity, carcinogenicity, or acute toxicity were identified, indicating that β-Amyrin could be compatible with long-term therapeutic strategies targeting axonal degeneration. In summary, the ADME and toxicity profiles suggest that β-Amyrin has stable systemic availability, a clean metabolic footprint, and a safety-oriented toxicological profile. While BBB permeability is modest, its capacity to influence peripheral SARM1-driven axonal degeneration underscores its viability as a natural neuroprotective candidate worthy of further experimental validation.

SARM1, the main effector of the Wallerian pathway of degeneration, has already received much interest as one of the key points of therapeutic intervention in axonal degeneration (PA Farraj and A Loreto 2025) Although the primary functioning of current pharmacological methods is the utilization of small-molecule inhibitors to block the NADase activity of the TIR domain, the structural complexity of SARM1, which allows it to switch between an auto-inhibited octamer form and an active enzyme, provides numerous sites of allosteric intervention.[17] In this work, we used phytochemical profiling together with modern quantum-chemical and structural modelling to discover β-Amyrin as an effective, dual-mechanism activator of this pathway. The analysis of the ethanolic extract of Centella asiatica by the use of GC-MS showed that it was a complex chemical environment[18], with β-Amyrin being one of the primary components (Peak Area: 3.52%; Retention Time: 27.049 min). This corresponds with the previous description of triterpenoid-rich fractions.[19,20] Despite the plethora of volatile derivatives, β-Amyrin was chosen as the first candidate because it had a known neuroprotective and anti-inflammatory profile.[21] We have performed electronic profiling analysis of β-Amyrin as a potential drug scaffold before docking it with Density Functional Theory (DFT).[22] Calculations showed that the molecule is chemically hard (HOMO-LUMO gap: 4.76 eV) and kinetically stable, with a chemical hardness of 2.38 Ev.[23] This stability is high, indicating that β-Amyrin is not readily metabolised, and this is a key requirement of a neuroprotective agent so that it remains in the physiological environment. The vibrational frequencies were analysed to validate the structural integrity of β-amyrin, showing strong agreement with experimental spectroscopic data reported in the literature. Specifically, the analysis confirmed the presence of the characteristic O–H stretching mode of the 3β-hydroxyl group in the 3600–3650cm^{-1}region. This alignment with established infrared (IR) profiles not only verifies the accuracy of the optimised geometry but also highlights the accessibility of the C-3 hydroxyl moiety.[24] These functional groups are widely recognised as important pharmacophoric elements in pentacyclic triterpenoids, contributing to hydrogen-bond donor/acceptor interactions with biological targets. A structural rationale for the activity of the compound was offered by the molecular docking simulations, which demonstrated that β-Amyrin has specific binding affinities to the two conformational states of SARM1. The ligand is much more likely to bind the auto-inhibited full-length octamer (PDB: 7CM6; -10.79 kcal/mol)[17] than the catalytic TIR domain (PDB: 8D0C; -9.45 kcal/mol).[25] This positive affinity supports the hypothesis of a metabolic biosensor, which posits that β-Amyrin stabilises the inactive position of the enzyme, but not only as a competitive inhibitor.[26] Our Molecular Electrostatic Potential (MEP) and atomic charge analyses provide support for the specific interplay of interactions that occur in docking. Analysis of Hirschfeld charges revealed the existence of a strong nucleophilic centre (C3-hydroxyl oxygen (-0.262e) in the structure. This oxygen atom in the catalytic TIR domain develops a significant hydrogen bond with Asn658, and the lipophilic backbone is involved in Pi-Alkyl interactions with His685. As His685 is the catalytic site necessary to cleave NAD^{+}[27,28], direct steric inhibition of this site will inhibit the enzyme, leading to metabolic collapse. At the same time, the non-polar triterpenoid core neutralises the Hirshfeld charges of C7 (0.000 e) and C17 (-0.050 e) are bound in an allosteric interface of the octamer with a hydrophobic

network of Leu334, Leu339, Leu377 and Arg376. This may indicate that β-Amyrin is a molecular lock that raises the energy barrier necessary to cause the conformational change leading to the death of the axons. To translate in silico results to clinical candidates, the bioavailability and toxicity have to be addressed, and β-Amyrin meets the requirements of most of the Lipinski Rule of Five (Lipinski *et al.,* 2001), except for the violation of lipophilicity (logP =7.0). Nonetheless, this high lipophilicity, which is verified by the fact that the strong alkyl C-H stretching vibrations (2915-2940 cm^{-1}) also occur in our spectrogram, is desirable for CNS penetration. ProTox-III prediction shows that β-Amyrin is capable of passing through the blood-brain barrier (BBB).[29] The rate of permeation is moderate, but probably is high enough to have therapeutic relevance, as in the case of SARM1-mediated pathology, it is common to initiate in distal axons.[30,31] Moreover, its safety profile is good; it belongs to Toxicity Class 6 (non-toxic), hepatotoxic and mutagenicity are not predicted and agree with earlier in vivo acute toxicity research of β-amyrin preparations.[32] All these results indicate that β-Amyrin acts through a complementary dual-action: by blocking the catalytic pore physically but stabilising the inactive octameric form selectively, which should be experimentally confirmed again in axonopathy models.

CONCLUSION

In summary, to our knowledge, this work offers the first in silico insights into how β-amyrin may target and structurally modulate the SARM1 execution machinery. Density Functional Theory calculations established the molecule's electronic stability, characterised by a wide HOMO-LUMO gap (4.76 eV) and a hard chemical character consistent with kinetic stability under physiological conditions. These quantum-chemical properties translated into two functionally distinct structural features: the C3-hydroxyl group, acting as a primary nucleophilic/H-bonding anchor, and the Δ12-olefinic bond, serving as a hydrophobic stabilising core. Molecular docking confirmed that these features drive a dual mechanism of action — β-amyrin sterically engaged the catalytic residue His685 within the TIR domain, while binding with higher affinity to the allosteric octameric interface (engaging Asn335 and Leu334); this finding is consistent with a model of structural stabilisation at the interface, which could theoretically act to restrict transitions toward the active state. Predicted ADMET properties, including blood-brain barrier permeability and a favourable safety margin, further support β-amyrin's suitability, despite several limitations associated with existing synthetic SARM1 inhibitors. We recommend that these findings be validated through in vitro NADase activity assays and cellular models of axonal degeneration, alongside experimental structural studies (e.g., X-ray crystallography or cryo-EM) to confirm the proposed allosteric binding mode. By generating this structurally grounded, computationally efficient evidence base ahead of costly experimental validation, this work contributes to Sustainable Development Goal 9 (Industry, Innovation, and Infrastructure), supporting innovation-driven infrastructure for early-stage neuroprotective drug discovery.

ACKNOWLEDGMENTS

The authors declare that they are thankful to Saveetha School of Engineering, SIMATS, for providing the necessary facilities to complete their targeted work.

CONFLICT OF INTERESTS

The authors declare that there is no conflict of interest.

AUTHORS CONTRIBUTION

The present work is related to *SDG-9: Industry, Innovation, and Infrastructure*. All the authors contributed significantly to this manuscript, participated in reviewing/editing and approved the final draft for publication. The research profile of the authors can be verified from their ORCID ids, given below:

Mohammad Umaid https://orcid.org/0009-0005-0087-4124
Mohammad Talib https://orcid.org/0009-0006-1232-4362
R. Vijayan http://orchid.org/0009-0005-9475-0025
S. Alagendran https://orcid.org/0009-0009-0749-7180
P. Arjun https://orcid.org/0000-0002-9731-1635
Ramalingam Karthik Raja https://orcid.org/0000-0003-3782-046X

Open Access: This article is distributed under the terms of the Creative Commons Attribution 4.0 International License (http://creativecommons.org/licenses/by/4.0/), which permits unrestricted use, distribution, and reproduction in any medium, provided you give appropriate credit to the original author(s) and the source, provide a link to the Creative Commons license, and indicate if changes were made.
Cite this article as: M. Umaid *et al.*, *Rasayan J. Chem.*, 19(4), 2553-2565(2026), https://doi.org/10.31788/RJC.2026.1949830

REFERENCES

1. Y. Cao and J. Yang, *Wiring the Nervous System: Mechanisms of Axonal and Dendritic Remodelling in Health and Disease*, pp.215–250(2024).
2. B. Beirowski, *Neurobiology of Disease*, **170**, 105751(2022), https://doi.org10.1016/j.nbd.2022.105751
3. P. Arthur-Farraj and A. Loreto, *Trends in Pharmacological Sciences*, **46(11)**, 11052025), https://doi.org10.1016/j.tips.2025.09.003.
4. E.L. Hopkins, W. Gu, B. Kobe and M.P. Coleman, *Frontiers in Molecular Biosciences*, **8**, 703532(2021)
5. T.D. Viet, T.D. Xuan and L.H. Anh, *Molecules*, **26(23)**, 7248(2021).
6. G.M. Morris, R. Huey, W. Lindstrom, M.F. Sanner, R.K. Belew, D.S. Goodsell and A.J. Olson, *Journal of Computational Chemistry*, **30(16)**, 2785(2009), https://doi.org10.1002/jcc.21256.
7. F. Neese, *WIREs Computational Molecular Science*, **12(5)**, e1606(2022), https://doi.org10.1002/wcms.1606.
8. A. Hellweg and D. Rappoport, *Physical Chemistry Chemical Physics*, **17(2)**, 1010(2015).
9. R. Vijayan, A.R. Kumar, A.H. Hirad, S. Selvaraj, U. Eswaranpillai, M. Rajendran, P. Karuppiah, S. Gurusamy and R.K. Raja, *Next Materials*, **12**, 101973(2026).
10. S.S. Pawar and S.H. Rohane, *Asian Journal of Research in Chemistry*, **14(1)**, 1(2021).
11. R. Ancuceanu, B.E. Lascu, D. Drăgănescu and M. Dinu, *Pharmaceutics*, **17(8)**, 1002(2025).
12. P. Banerjee, E. Kemmler, M. Dunkel and R. Preissner, *Nucleic Acids Research*, **52(W1)**, W513(2024), https://doi.org10.1093/nar/gkae303.
13. Y. Jiang, T. Liu, C.-H. Lee, Q. Chang, J. Yang and Z. Zhang, *Nature*, **588(7839)**, 658(2020).
14. J.T. James and I.A. Dubery, *Molecules*, **14(10)**, 3922(2009).
15. I.B. Ganie, Z. Ahmad, A. Shahzad, A. Zaushintsena, O. Neverova, S. Ivanova, A. Wasi and S. Tahseen, *Plants*, **11(21)**, 2928(2022).
16. V.R. Askari, N. Fereydouni, V.B. Rahimi, N. Askari, A.H. Sahebkar, P. Rahmanian-Devin and A. Samzadeh-Kermani, *Biomedicine & Pharmacotherapy*, **101**, 438(2018).
17. M.S. Hossain, S. Hasnat, S. Akter, M.M. Mim, A. Tahcin, M. Hoque, D. Sutradhar, M.A.A. Keya, N.R. Sium and S. Hossain, *Frontiers in Pharmacology*, **15**, 1465827(2024).
18. Y. Shi, P.S. Kerry, J.D. Nanson, T. Bosanac, Y. Sasaki, R. Krauss, F.K. Saikot, S.E. Adams, T. Mosaiab and V. Masic, *Molecular cell*, **82(9)**, 1643(2022).
19. S. Horsefield, H. Burdett, X. Zhang, M.K. Manik, Y. Shi, J. Chen, T. Qi, J. Gilley, J.-S. Lai, M.X. Rank, L.W. Casey, W. Gu, D.J. Ericsson, G. Foley, R.O. Hughes, T. Bosanac, M. Von Itzstein, J.P. Rathjen, J.D. Nanson, M. Boden, I.B. Dry, S.J. Williams, B.J. Staskawicz, M.P. Coleman, T. Ve, P.N. Dodds and B. Kobe, *Science*, **365(6455)**, 793(2019), https://doi.org10.1126/science.aax1911.
20. K. Essuman, D.W. Summers, Y. Sasaki, X. Mao, A. DiAntonio and J. Milbrandt, *Neuron*, **93(6)**, 1334(2017).
21. C.A. Lipinski, F. Lombardo, B.W. Dominy and P.J. Feeney, *Advanced Drug Delivery Reviews*, **23(1–3)**, 3(1997).
22. A. Daina, O. Michielin and V. Zoete, *Scientific Reports*, **7(1)**, 42717(2017).
23. R. Vijayan, C. Veeramani, M.A. Alsaif, K.S. Al-Numair, A. Thanikasalam, A.R. Kumar, S. Selvaraj, P. Velmurugan and R.K. Raja, *Next Materials*, **12**, 102152(2026).

[RJC-9830/2026]